AMERICAN SCIENTIFIC PUBLISHERS

Science of Advanced Materials
Vol. 8, pp. 884–890, 2016
www.aspbs.com/sam

ARTICLE

Low Energy BCl_3 Plasma Doping of Few-Layer Graphene

Viet Phuong Pham[1], Doo San Kim[2], Ki Seok Kim[2], Jin Woo Park[2], Kyung Chae Yang[2], Se Han Lee[1], Geun Young Yeom[1,2,*], and Kyong Nam Kim[2,*]

[1] *SKKU Advanced Institute of Nano Technology (SAINT), Sungkyunkwan University (SKKU), Suwon, Gyeonggi-do 440-746, Republic of Korea*
[2] *School of Advanced Materials Science and Engineering, Sungkyunkwan University (SKKU), Suwon, Gyeonggi-do 440-746, Republic of Korea*

ABSTRACT

In this paper, we use low energy BCl_3 plasma for the doping of graphene, and investigate its effect on graphene sheet resistance. In particular, for few-layer graphene, we use a cyclic trap-doping technique to control the dopants between the graphene layers. By using the cyclic tra-doping with the low energy BCl_3 plasma, we obtain significant reduction of sheet resistance (∼75%), while maintaining high optical transparency, flexibility, conductivity, and thermal stability. Raman data show that the graphene layers are *p*-type doped with no noticeable damage during the doping. By optimizing the doping condition, we obtain sheet resistance and optical transmittance of BCl_3 doped trilayer graphene of 100 Ω/sq and 92% at 550 nm, respectively, which is very compatible with flexible display devices.

KEYWORDS: BCl_3, Plasma Doping, Trapped-Doping, Multilayer Graphene, Low Damage.

1. INTRODUCTION

Graphene that consists of a few layers of graphite in which each carbon atom possesses a sp^2 hybridization has attracted huge attention, due to its extraordinary mechanical and electrical properties.[1–7] Some of its key properties are suitability for transparent conductive films of high conductivity, high transparency, and excellent flexibility; and therefore, graphene has been studied as a possible replacement for indium tin oxide (ITO).[8–11, 13–15] For this purpose, many approaches and much progress have been reported on the synthesis of large area graphene using chemical vapor deposition (CVD).[9–11, 13–16] However, graphene grown by CVD has shown higher sheet resistance compared to ideal graphene, and variation with growth conditions, due to defects in the crystal, such as wrinkles, domains, and grain boundaries.[9] Therefore, the relatively high sheet resistance has been a bottleneck for the application to transparent conductive films.

For these reasons, researchers have tried to improve the sheet resistance by various doping methods, which have included chemical,[11, 12, 17] plasma,[18–20] and photochemical methods.[20] However, many problems remain unsolved, such as the much higher sheet resistance than that of ITO at similar optical transmittance conditions, transmittance degradation during chemical doping, thermal instability, and serious damage during plasma doping. For example, in the case of wet chemical doping, Gunes et al. showed the possibility of obtaining low sheet resistance by $AuCl_3$ chemical doping, and obtained 54 Ω/sq. for four-layer graphene.[11] However, their doping process showed a relatively poor transmittance of 85%. Li et al. used a photochemical doping process to reduce the sheet resistance; however, it increased by about 3 orders of magnitude by interrupting the conducting system of the graphene, and introducing damage-inducing scattering centers.[20] Other researches on chemical doping have also been carried out to improve the electrical conductivities of graphene transparent conductors; however, the sheet resistances were still high, or optical transmittance was low in performance for industrial applications.[17, 21–25]

Plasma doping has also been investigated to improve graphene properties. Among the various gases, Cl_2 is studied as one of the most controllable graphene doping techniques.[19] In general, plasma doping can result in the reduction of sheet resistance, without sacrificing optical transmittance. However, in the case of plasma doping by conventional plasma methods, the decrease of sheet resistance is limited, due to the damage of the graphene surface during the plasma exposure, resulting from energetic particle bombardment during the processing. In our previous study, we introduced a low damage plasma doping by

*Authors to whom correspondence should be addressed.
Emails: gyyeom@skku.edu, knam1004@gmail.com
Received: 17 August 2014
Accepted: 1 February 2015

using a double mesh grid between the plasma source and the substrate, and by using Cl_2 as the doping gas.[26] Also, to more effectively confine the chlorine dopants in graphene layers, we used a cyclic trap-doping technique, where the chlorine dopants were trapped between the graphene layers, and obtained a significant decrease of graphene sheet resistance of about 88%, without changing the optical transmittance, with long-term thermal stability.

In this study, we conduct doping of few-layer graphene using a BCl_3 plasma instead of Cl_2 plasma, using similar doping techniques to the previous study.[26] In the doping using BCl_3, boron is the substitutional hole dopant (not recommended, because of forming defects in the graphene layer),[18, 27–31] and can remove oxygen on the graphene surface, by forming volatile $BOCl_x$. Chlorine atom is also a hole dopant, by forming C–Cl bond on the graphene surface. To effectively adsorb the radicals on the graphene surface without damaging the graphene surface by the plasma, we used a pre-doping technique in addition to the previous doping techniques, where we additionally doped the graphene on Cu foil before transfer to the substrate, in addition to the conventional doping conducted after the transfer to the substrate. By using these techniques, we investigated the effect of BCl_3 plasma doping on the characteristics of few-layer graphene.

2. EXPERIMENTAL DETAILS

We synthesized monolayer graphene film on Cu foil by a low-pressure chemical vapor deposition (LPCVD) method at 1050 °C, by a gas flow of H_2/CH_4 (10/20 sccm) for 30 min. The details of the graphene growth method can be found elsewhere.[26] The graphene grown on Cu foil was transferred to substrates by spin coating using PMMA, then by dipping in an $FeCl_3$ copper etchant solution for 45 min on a hot plate (45 °C) to dissolve Cu foil, and by transferring the PMMA-coated graphene on PET substrates and SiO_2/Si substrates. Finally, the PMMA on graphene was removed by acetone (10 min), IPA (10 min) and DI water (10 min). For a few-layer graphene on the substrate, the PMMA coated graphene was transferred again on the substrates with previous graphene, and the PMMA on the fresh-coated graphene was removed; and this sequence was repeated for a few-layer graphene on PET substrates and SiO_2/Si substrates.

For the BCl_3 plasma doping, we used a conventional inductively-coupled plasma (ICP) source, with a dual mesh assembly inserted between the plasma source and the substrate. The dual mesh grid used in this study has geometrical transparency of more than 62%, with small mesh aperture size of ~8 μm, and two grids separated by 2 cm from each other. This mesh grid behaved like a solid

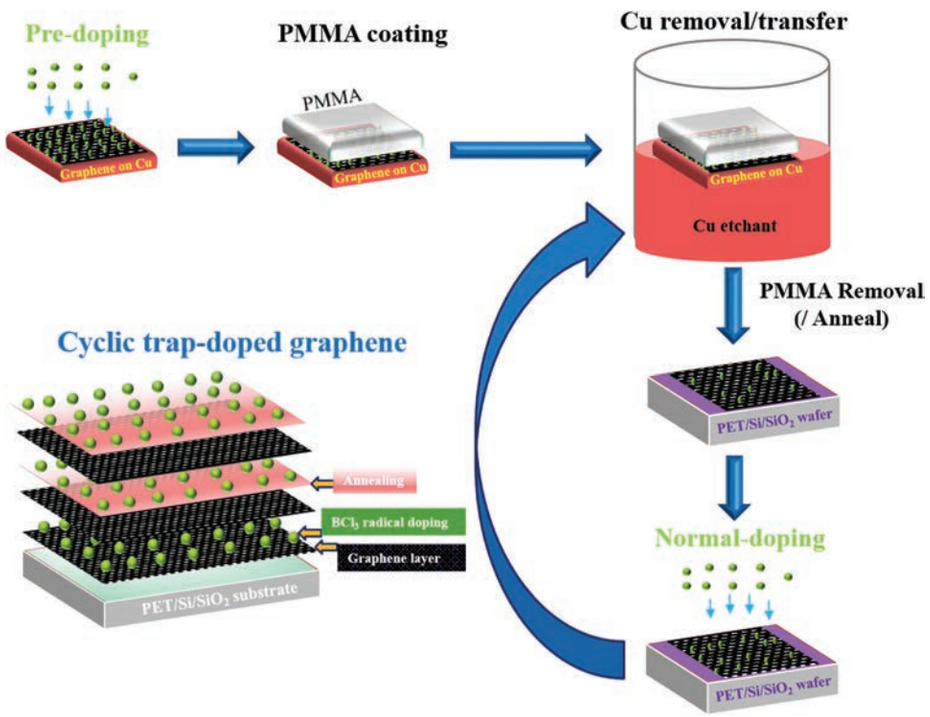

Fig. 1. Graphene doping techniques used in this experiment. The graphene on Cu foil was pre-doped with BCl_3 before transfer to wafer. After transfer to the substrates, the graphene on substrates was normal-doped with BCl_3 again. For bi-layer graphene, the second layer pre-doped graphene was transferred to the substrate with the pre- and normal-doped first layer graphene. The dopant trapped bi-layer graphene was annealed at 230 °C for 30 min in a vacuum furnace. For the second cyclic trap-doping, the same sequence was repeated on the bi-layer graphene for the tri-layer graphene formation.

potential surface in plasma, and efficiently confined the plasma; therefore, we could realize chlorine plasma doping with extremely low damage. The BCl_3 plasma was sustained at 13.56 MHz RF power of 38 W, and pressure of 8 mTorr. The BCl_3 gas flow rate was kept at 20 sccm. The BCl_3 doping was carried out for 30–180 sec. The graphene films were inserted in the processing chamber using a load-lock system without breaking the vacuum, and the substrate was cooled at temperature of 15 °C with a chiller.

Figure 1 shows the graphene doping techniques used in this experiment. As a pre-doping technique, we doped the graphene on Cu foil by BCl_3 plasma before transfer to the substrate. For normal doping, we performed plasma doping on the graphene transferred to the substrate. We used the pre-doping to maximize the doping concentration on the graphene surface, in addition to the conventional normal doping that we conducted after the transfer to the substrate. Also, for few-layer graphene, as the cyclic trap-doping, we conducted the pre-doping and normal doping of each monolayer graphene during the repeated graphene transfer to the substrate. During the cyclic BCl_3 radical doping, just after the transfer of each graphene layer, we annealed the graphene in a vacuum furnace at 250 °C for the SiO_2 substrate, and at 230 °C for the PET film, from 30 min to 6 h.

We measured the sheet resistance of graphene films on PET substrates or Si/SiO_2 substrate using a sheet resistance meter (Dasoleng, FPP-2400) at room temperature. UV-Vis-NIR spectroscopy (Shimadzu, 3600) and Raman spectroscopy (RM-1000 Invia, Renishaw) with excitation energy of 2.41 eV (514 nm, Ar ion laser) were used to characterize the optical properties, and to investigate the damage produced by plasma on the graphene films, respectively. The bending test of the graphene coated on PET was carried out under the bending condition of 5.0 mm curvature radius and bending frequency of 1 Hz, using an in-house bending test machine.

3. RESULTS AND DISCUSSION

First, we investigated the sheet resistance of the monolayer graphene after various doping techniques by the BCl_3 plasma as a function of plasma exposure time. Figure 2 shows the results. The BCl_3 plasma was generated at 38 W of rf power with 20 sccm, 8 mTorr BCl_3. We doped the monolayer graphene to the graphene on Cu foil with the BCl_3 plasma before transfer to the SiO_2/Si substrate (pre-doping), and doped the monolayer graphene with the BCl_3 plasma after transfer to the substrate (normal doping), or we doped the graphene both before and after the transfer to the substrate. Figure 2 shows that the monolayer graphene transferred to the substrate without any doping showed about 657 Ω/sq of sheet resistance. In the case of the normal doping, the sheet resistance of the monolayer graphene decreased with the increase of doping exposure time up to 120 sec, and further increase of doping

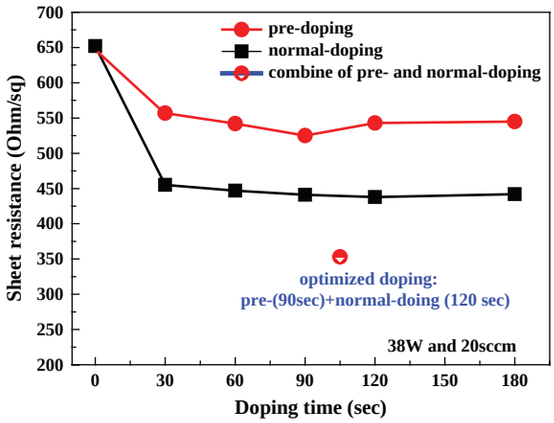

Fig. 2. Sheet resistance of the monolayer graphene after various doping techniques by BCl_3 plasma, as a function of the plasma exposure time. The BCl_3 plasma was generated at 38 W of rf power with 20 sccm, 8 mTorr BCl_3. The monolayer graphene was doped to the graphene on Cu foil with the BCl_3 plasma before transfer to the substrate (pre-doping), after transfer to the substrate (normal doping), or both before and after transfer to the substrate. The sheet resistances were measured after transfer to the SiO_2/Si wafers.

exposure time slightly increased the sheet resistance. We believe the decrease of graphene sheet resistance after the BCl_3 plasma exposure to be related to the *p*-type doping effect by forming C–Cl bonds. The boron in the BCl_3 plasma can remove oxygen on the graphene surface, but its effect is not clear at this time. The slight increase of sheet resistance after 120 sec appears to be related to the slight physical damage on the graphene surface due to extended BCl_3 plasma exposure. We observed similar decrease of sheet resistance with the plasma exposure time for the pre-doped graphene. For the pre-doped graphene, the dopants can wash away during the transfer to the SiO_2/Si substrate; however, as Figure 2 shows, the sheet resistance also decreased with the increase of plasma exposure time until 90 sec (554 Ω/sq), due to the C–Cl bonds remaining, even after transfer to the substrate. However, the sheet resistance of the pre-doped graphene was generally higher than that of the normal doped graphene, due to the removal of most of the chlorine dopant on the graphene surface during the transfer process. When we performed the optimized pre-doping condition of 90 sec and the optimized normal doping condition of 120 sec on the same monolayer graphene, we obtained the lowest sheet resistance of about 353 Ω/sq for monolayer graphene.

The dopants adsorbed on the graphene surface can donate holes by forming C–Cl bonds on the graphene surface. However, these dopants may easily vaporize by subsequent device processing, such as thermal annealing. We investigated the thermal stability of graphene doped with BCl_3 plasma by annealing at 230 °C in a vacuum furnace up to 6 h, and Figure 3 shows the results. As the doped monolayer graphene, we used the graphene doped with the optimized doping of pre-doping (90 sec)

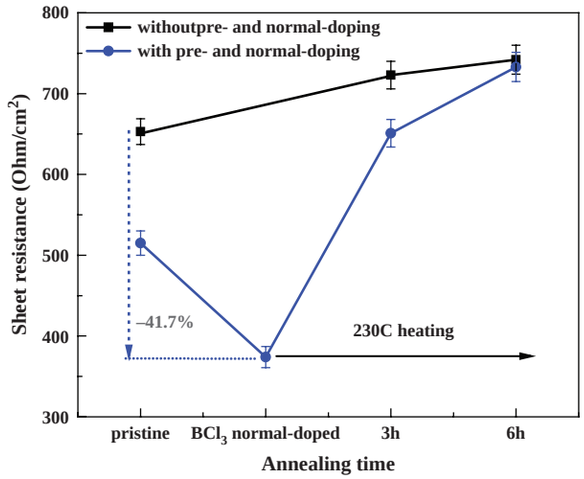

Fig. 3. Change of sheet resistance of the undoped monolayer graphene and monolayer graphene doped with the optimized doping of pre-doping (90 sec) and normal doping (120 sec), as a function of annealing time. The annealing was conducted at 230 °C in a vacuum furnace.

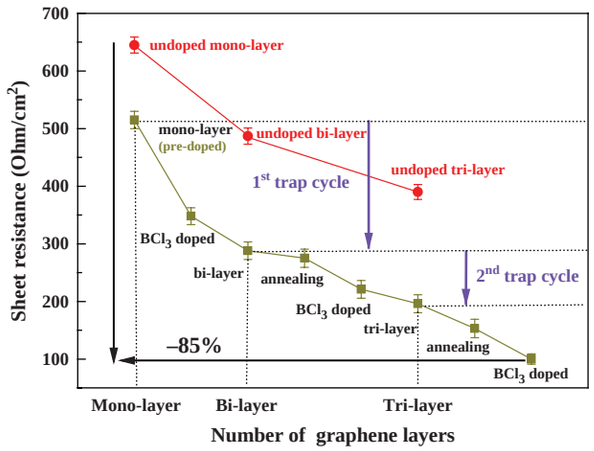

Fig. 4. Change of sheet resistance through cyclic trap-doping, which includes the first cycle of trap-doping (BCl_3 doping, transfer of second graphene layer, annealing), and second cycle of trap-doping (second cycle of BCl_3 doping, transfer of third graphene layer, annealing).

and normal doping (120 sec), and compared the sheet resistance of the doped graphene with that of undoped graphene. As Figure 3 shows, the sheet resistance of the undoped graphene increased slightly by about 12% from 653 to 742 Ω/sq by annealing for 6 h. However, in the case of the doped graphene, the sheet resistance increased significantly with the increase in annealing time, from 374 to 733 Ω/sq by annealing for 6 h; therefore, after 6 h, the sheet resistance of the doped graphene increased to close to that of undoped graphene.

Therefore, for the BCl_3 plasma doping to few-layer graphene, we also introduced the cyclic trap-doping investigated in our previous study to maintain the thermal stability of the doped graphene.[26] Figure 1 shows the doping sequence. For the first cyclic trap-doping, after the pre-doping to the graphene on Cu foil and the normal doping with the BCl_3 plasma on the first graphene layer on the substrate, we transferred the second layer pre-doped graphene to the graphene substrate for trapping of the dopants between the first and second layers. We annealed the dopant trapped bi-layer graphene at 230 °C for 30 min in a vacuum furnace. For the second cyclic trap-doping, we repeated the same sequence on the bi-layer graphene for the tri-layer graphene formation. Figure 4 shows the sheet resistance measured after each step from the monolayer to the tri-layer graphene formation. For undoped bi-layer graphene and undoped tri-layer graphene, the sheet resistances are 487 and 390 Ω/sq, respectively; while those of the trap-doped bi-layer graphene and tri-layer graphene are 221 and 100 Ω/sq (a decrease of ~85% compared to the undoped monolayer graphene, and a decrease of ~75% compared to the undoped tri-layer graphene) after the additional BCl_3 plasma doping, respectively. Therefore, the sheet resistance of the cyclic trap-doped graphene decreased not only with the increase of graphene layers, but also with the increase of each step, due to the formation of C–Cl bonds between the graphene layers, in addition to the graphene surface. The annealing after the BCl_3 plasma doping decreased the sheet resistance further, possibly due to the more stable C–Cl bond formation between the graphene layers by the trapped chlorine atoms.

To investigate possible structural damage to the graphene during the BCl_3 plasma doping used in the experiment, we measured Raman spectra of the graphene layers exposed to the BCl_3 plasma, and compared the results with those of graphene layers not exposed to the plasma. Figures 5(a) and 6(a) show Raman spectra of the monolayer graphene with/without the optimized doping of pre-doping (90 sec) + normal doping (120 sec), and the tri-layer graphene with/without doping with the cyclic doping described in Figure 3, respectively. Figures 5(a) and 6(a) show that the D peak intensities (located near 1350 cm^{-1}) of the monolayer graphene and tri-layer graphene were extremely low for both undoped pristine graphene layers and doped graphene layers, which indicated no noticeable structural damage to the graphene after the BCl_3 plasma doping for both the monolayer graphene and tri-layer graphene investigated in this study. In addition, Figures 5(b) and (c) and Figures 6(b) and (c) show the G and 2D peak intensities corresponding to Figures 5(a) and 6(a), respectively. These show blue shifts of the G peak of about 1 and 3 cm^{-1}, and blue shifts of the 2D peak of about 4 and 7 cm^{-1} after the doping of monolayer graphene and the cyclic doping of tri-layer graphene, respectively, indicating hole doping after the BCl_3 plasma doping.

High optical transmittance of the graphene layer, in addition to low sheet resistance, is important for application to transparent electrodes. Therefore, we measured the optical transmittance of the mono-, bi-, and tri-layer graphene on 100 μm thick PET substrates doped

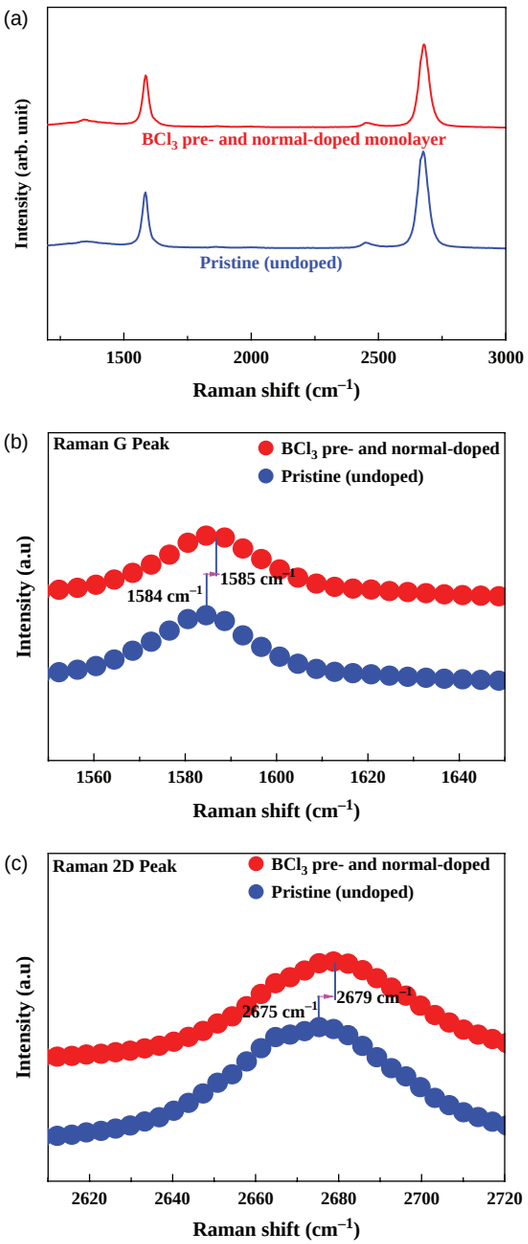

Fig. 5. (a) Raman spectra data for monolayer graphene before and after the optimized doping of pre-doping (90 sec) and normal doping (120 sec) using the low energy BCl_3 plasma. The BCl_3 plasma was generated at 38 W of rf power with 20 sccm, 8 mTorr BCl_3. (b) Zoom-in spectrum of the Raman G peak before/after the BCl_3 plasma doping. (c) Zoom-in spectrum of the Raman 2D peak before/after the BCl_3 plasma doping.

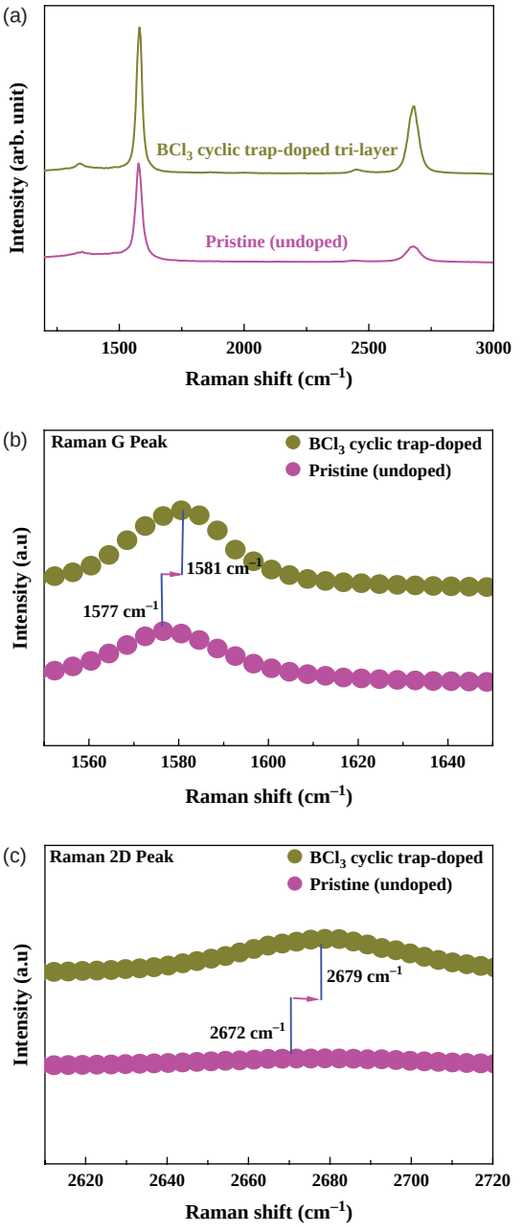

Fig. 6. (a) Raman spectra data for tri-layer graphene before and after the cyclic trap-doping using the low energy BCl_3 plasma. The BCl_3 plasma was generated at 38 W of rf power with 20 sccm, 8 mTorr BCl_3. (b) Zoom-in spectrum of the Raman G peak before/after the BCl_3 plasma doping. (c) Zoom-in spectrum of the Raman 2D peak before/after the BCl_3 plasma doping.

with BCl_3 plasma, and Figure 7 shows the results. The mono-layer graphene doped with the optimized doping (pre-doping 90 sec + normal doping 120 sec) showed a high transmittance of ~97% at 550 nm. For the bi-layer graphene and tri-layer graphene doped by the cyclic trap-doping using the BCl_3 plasma, we measured the optical transmittance of 94.5 and 92% at 550 nm, respectively. One monolayer graphene absorbs 2.3~2.4% at 550 nm; therefore, the optical transmittances of the doped mono-, bi-, and tri-layer graphene that we observed in the experiment were similar to those of undoped pristine mono-, bi-, and tri-layer graphene.

Electrical stability of the electrodes during bending is important for flexible transparent electrodes. We measured the sheet resistances of the undoped monolayer graphene and the doped mono-, bi-, and tri-layer graphene on PET

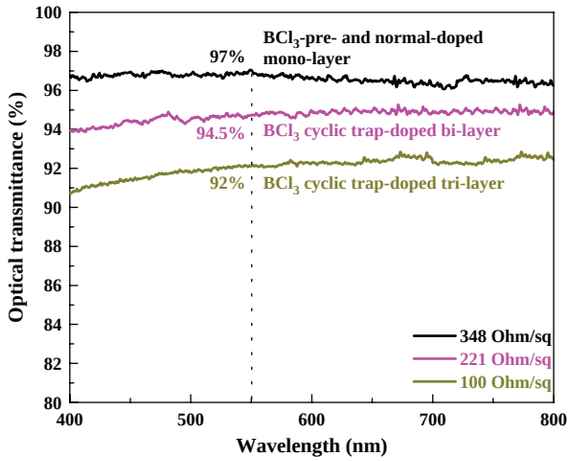

Fig. 7. Optical transmittance of the mono-, bi-, and tri-layer graphene on 100 μm thick PET substrates doped with the BCl_3 plasma, and measured using UV-Vis-NIR spectroscopy. PET substrate itself showed 100% optical transmittance.

substrates as a function of bending cycles, and Figure 8 shows the results. We bent the graphene on PET substrates with a 5.0 mm curvature radius for 800 cycles at a frequency of 1 Hz. The figure shows that in the case of undoped pristine monolayer graphene, the sheet resistance continuously increased by about 38% from ~650 to ~900 Ω/sq after 800 bending cycles, possibly due to defect formation on the graphene. In the case of monolayer graphene doped with optimized doping, even though the amount of sheet resistance increase was lower than that of the undoped monolayer graphene, the increased percentage of the sheet resistance was similar at 37%, increasing from ~350 to ~480 Ω/sq after 800 bending cycles. But in the case of bi- and tri-layer graphene on PET substrates doped by cyclic trap-doping, the sheet resistances did not change noticeably until 800 bending cycles, possibly due to the stronger and stable C–Cl bonding between graphene layers.

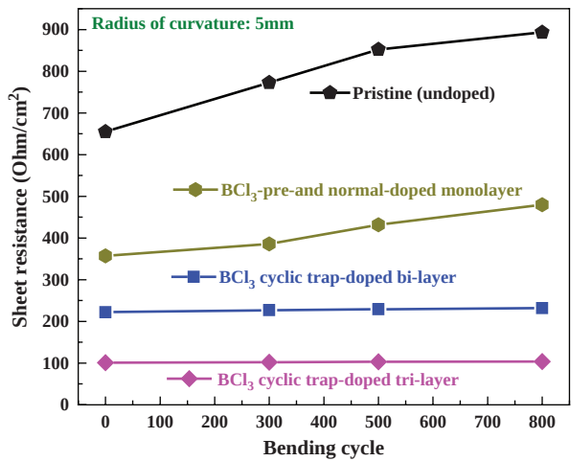

Fig. 8. Sheet resistances of the undoped monolayer graphene and the doped mono-, bi-, and tri-layer graphene on PET substrates, measured as a function of bending cycles. The graphene on PET substrates was bent with a 5.0 mm curvature radius, at a frequency of 1 Hz.

4. CONCLUSION

In this study, we conducted doping of a few-layer graphene using a low energy BCl_3 plasma, and with doping techniques such as pre-doping and cyclic trap-doping, and investigated the effect of BCl_3 plasma doping on the characteristics of few-layer graphene. For the low energy BCl_3 plasma used in the experiment, we observed no noticeable damage on the graphene during plasma doping, due to the dual mesh grid installed between the plasma and substrate. When we used this BCl_3 plasma for the doping of graphene, the sheet resistance of monolayer graphene decreased about 53% from 650~ to ~350 Ω/sq, after the optimized graphene doping composed of pre-doping (90 sec) and normal doping (120 sec). However, the sheet resistance of the doped graphene increased close to undoped graphene after annealing at 230 °C for 6 h, possibly due to the easy vaporization of doped Cl on the graphene surface. For a few-layer graphene, by using cyclic trap-doping, we could significantly reduce the sheet resistance, without changing with annealing. With tri-layer graphene on PET substrate, after the cyclic trap-doping, we obtained 100 Ω/sq of sheet resistance while keeping the optical transmittance of 92% at 550 nm, similar to that of undoped tri-layer graphene. The bending of 800 cycles did not noticeably change the sheet resistance of the few-layer graphene doped with cyclic trap-doping.

Acknowledgments: This study was supported by the Nano Material Technology Development Program, through the National Research Foundation of Korea, funded by the Ministry of Education, Science and Technology (2012M3A7B4035323); and was also supported by the Ministry of Trade, Industry and Energy (10048504), and the Korea Semiconductor Research Consortium support program for the development of the future semiconductor device.

References and Notes

1. K. S. Novoselov, A. K. Geim, S. V. Morozov, Y. Zhang, S. V. Dubonos, I. V. Grigorieva, and A. A. Firsov, *Science* 306, 666 (**2004**).
2. K. S. Novoselov, A. K. Geim, S. V. Morozov, D. Jiang, M. I. Katsnelson, I. V. Grigorieva, S. V. Dubonos, and A. A. Firsov, *Nature* 438, 197 (**2005**).
3. C. R. Dean, A. F. Young, C. Lee, L. Wang, S. Sorgenfrei, K. Watanabe, T. Taniguchi, P. Kim, K. L. Shepard, and J. Hone, *Nature Nanotech.* 5, 722 (**2010**).
4. F. Wang, Y. B. Zhang, C. Tian, C. Girit, A. Zettl, M. Crommie, and Y. R. Shen, *Science* 320, 206 (**2008**).
5. J. H. Park, W. Jung, D. Cho, J. T. Seo, Y. Moon, S. H. Woo, C. Lee, and C. Y. Park, *Appl. Phys. Lett.* 103, 171609 (**2013**).
6. A. K. Geim, *Science* 324, 1530 (**2009**).
7. A. K Geim and K. S. Novoselov, *Nat. Mater.* 6, 183 (**2007**).
8. D. Langley, G. Giusti, C. Mayousse, C. Celle, D. Bellet, and J. P. Simonato, *Nanotechnology* 24, 452001 (**2013**).

9. S. K. Bae, H. K. Kim, Y. B. Lee, X. F. Yu, J. S. Park, Y. Zheng, J. Balakrishnan, T. Lei, H. R. Kim, Y. I. Song, Y. J. Kim, K. S. Kim, B. Ozyilmaz, J. H. Ahn, B. H. Hong, and S. Iijima, *Nature Nanotech.* 5, 574 **(2010)**.
10. C. Mattevi, H. W. Kim, and M. Chhowalla, *J. Mater. Chem.* 21, 3324 **(2011)**.
11. F. Gunes, H. J. Shin, C. Biswas, G. H. Han, E. S. Kim, S. J. Chae, J. Y. Choi, and Y. H. Lee, *ACS Nano* 4, 4595 **(2010)**.
12. J. Zheng, H. T. Liu, B. Wu, C. A. Di, Y. L. Guo, T. Wu, G. Yu, Y. Q. Liu, and D. B. Zhu, *Scientific Report* 2, 662 **(2012)**.
13. U. N. Maiti, W. J. Lee, J. M. Lee, Y. T. Oh, J. Y. Kim, J. E. Kim, J. W. Shim, T. H. Han, and S. O. Kim, *Adv. Mater.* 26, 40 **(2014)**.
14. D. S. Hecht, L. B. Hu, and G. Irvin, *Adv. Mater.* 23, 1482 **(2011)**.
15. X. Huang, C. L. Tan, Z. Yin, and H. Zhang, *Adv. Mater.* 26, 2185 **(2014)**.
16. M. Wang, S. K. Jang, W. J. Jang, M. W. Kim, S. Y. Park, S. W. Kim, S. J. Kahng, J. Y. Choi, R. S. Rouff, Y. J. Song, and S. J. Lee, *Adv. Mater.* 25, 2746 **(2013)**.
17. H. Liu, Y. Liu, and D. Zhu, *J. Mater. Chem.* 21, 3335 **(2011)**.
18. X. Zhang, A. Hsu, H. Wang, Y. Song, J. Kong, M. S. Dresselhaus, and T. Palacios, *ACS Nano* 7, 7262 **(2013)**.
19. J. Wu, L. Xie, Y. G. Li, H. L. Wang, Y. Ouyang, J. Guo, and H. Dai, *J. Am. Chem. Soc.* 13, 19668 **(2011)**.
20. B. Li, L. Zhou, D. Wu, H. Peng, K. Yan, and Z. F. Liu, *ACS Nano* 5, 5957 **(2011)**.
21. Y. Wang, C. Di, Y. Liu, H. Kajiura, S. Ye, L. Cao, D. Wei, H. Zhang, Y. Li, and K. Noda, *Adv. Mater.* 20, 4442 **(2008)**.
22. Q. B. Zheng, M. M. Gudarzi, S. J. Wang, Y. Geng, Z. Li, and J. K. Kim, *Carbon* 49, 2905 **(2011)**.
23. P. Barpanda, G. Fanchini, and G. G. Amatucci, *Carbon* 49, 2538 **(2011)**.
24. Q. Zheng, W. H. Ip, X. Lin, N. Yousefi, K. K. Yeung, Z. Li, and J. K. Kim, *ACS Nano* 7, 6039 **(2011)**.
25. Q. Zheng, Z. Li, J. Yang, and J. K. Kim, *Prog. Mater. Sci.* 64, 200 **(2014)**.
26. V. P. Pham, K. N. Kim, M. H. Jeon, K. S. Kim, and G. Y. Yeom, *Nanoscale* 6, 15301 **(2014)**.
27. H. Wang, Y. Zhou, D. Wu, L. Liao, S. Zhao, H. Peng, and Z. Liu, *Small* 9, 1316 **(2013)**.
28. Z. S. Wu, W. Ren, L. Xu, F. Li, and H. M. Cheng, *ACS Nano* 5, 5463 **(2011)**.
29. T. Lin, F. Huang, J. Liang, and Y. Wang, *Energy Environ. Sci.* 4, 862 **(2011)**.
30. T. Wu, H. Shen, L. Sun, B. Cheng, B. Liu, and J. Shen, *New J. Chem.* 36, 1385 **(2012)**.
31. Z. H. Sheng, H. L. Gao, W. J. Bao, F. B. Wang, and X. H. Xia, *J. Mater. Chem.* 22, 390 **(2012)**.